

Abstract. We present HST WFPC2 and ground-based images of the low surface brightness dwarf *Irr/Sph* galaxy KKR 25 in Draco. Its colour-magnitude diagram shows red giant branch stars with the tip at $I = 22^m32$, and the presence of some blue stars. The derived true distance modulus, $26^m35 \pm 0^m14$, corresponds to linear distances of KKR 25 from the Milky Way and from the Local Group centroid of 1.86 and 1.79 Mpc, respectively. The absolute magnitude of the galaxy, $M_V = -10.48$, its linear diameter (0.54 Kpc) and central surface brightness ($\Sigma_{0,V} = 24^m0 \pm 0^m2/\square''$) are typical of other *dIrr/dSphs* in the Local Group. Being situated just beyond the radius of the zero-velocity surface of the Local Group, KKR 25 moves away from the LG centroid at a velocity of $V_{LG} = +72$ km/s.

Key words: galaxies: dwarf — galaxies: distances

A new galaxy near the Local Group in Draco [★]

I.D.Karachentsev¹, M.E.Sharina¹, A.E.Dolphin², D.Geisler³, E.K.Grebel⁴, P.Guhathakurta^{5**}, P.W.Hodge⁶, V.E.Karachentseva⁷, A.Sarajedini⁸, and P.Seitzer⁹

¹ Special Astrophysical Observatory, Russian Academy of Sciences, N.Arkhiz, KChR, 369167, Russia,

² Kitt Peak National Observatory, National Optical Astronomy Observatories, P.O. Box 26732, Tucson, AZ 85726, USA

³ Departamento de Fisica, Grupo de Astronomia, Universidad de Concepcion, Casilla 160-C, Concepcion, Chile

⁴ Max-Planck-Institut für Astronomie, Königstuhl 17, D-69117 Heidelberg, Germany

⁵ UCO/Lick Observatory, University of California at Santa Cruz, Santa Cruz, CA 95064, USA

⁶ Department of Astronomy, University of Washington, Box 351580, Seattle, WA

⁷ Astronomical observatory of Kiev University, 04053, Observatorna 3, Kiev, Ukraine

⁸ Department of Astronomy, University of Florida, Gainesville, FL 32611, USA

⁹ Department of Astronomy, University of Michigan, 830 Dennison Building, Ann Arbor, MI 48109, USA

Received: 31 July 2001/Accepted 12 September 2001

1. Introduction

Among the faintest dwarf irregular (dIrr) galaxies in the Local Group, there are galaxies that may be in transition from dIrrs to dwarf spheroidals (dSphs): Phoenix ($M_V = -9.8$) and LGS 3 ($M_V = -10.5$). These galaxies contain prominent old populations reminiscent of dSphs, but also some recent star formation as indicated by young blue stars and have HI associated with them, which is characteristic for dIrrs. They are therefore classified as dIrr/dSphs (Grebel 2000). The discovery of Antlia dwarf (Whiting et al. 1997) with $M_V = -10.7$ at a distance of $D = 1.32$ Mpc, shows that such extremely faint bluish galaxies of regular shape may also occur outside the Local Group. A detailed studying of these tiny transient objects is very important to understand their origin and evolution.

The detection of low surface brightness galaxies with an absolute magnitude of about -10^m , situated between galaxy groups, is a complicated observational task. Recent all-sky searches for nearby dwarf galaxies made on the POSS-II and ESO/SERC plates by Karachentseva & Karachentsev (1998), Karachentseva et al. (1999,2000), and Karachentsev et al. (2000) has led to the discovery of ~ 600 objects mainly of low surface brightness. One object from these lists, KKR 25, (Karachentseva et al. 1999) is considered in the present Note.

KKR 25 has an apparent size of $1'.1 \times 0'.65$ and is located next to a luminous red foreground star. In its direc-

tion Huchtmeier et al. (2000) detected HI emission with a heliocentric radial velocity $V_h = (-135 \pm 2)$ km/s and a linewidth $W_{50} = 14$ km/s, which was attributed to local Galactic hydrogen. The first large-scale image of KKR 25 was obtained with the 6-m telescope (SAO, Russia) in the R and I bands with a $1''.1$ seeing (FWHM) on June 18, 1999. The R image, presented in Fig.1, shows that the galaxy is well resolved into stars. The brightest stars in the galaxy body have a red color $(R - I) \sim 0.7$ and an apparent magnitude $m_I \sim 22^m$. The preliminary distance estimate, mentioned by Karachentsev & Makarov (2001), yields for KKR 25 $D \sim 1.5$ Mpc. Due to this very close distance, we included KKR 25 in our ongoing Hubble Space Telescope snapshot survey.

2. HST WFPC2 observations and data reduction

Observations of KKR 25 with the Hubble Space Telescope WFPC2 were obtained on May 25, 2001 as part of the HST snapshot survey of probable nearby galaxies (GO program 8601, PI: P.Seitzer). The galaxy was imaged in F606W and F814W with exposure times of 600^s each, with the galaxy center located in the WF3 chip. Fig. 2 shows the galaxy image on this chip resulting from the combination of both filters to remove cosmic rays.

The photometric pipeline used for the snapshot survey has been described in detail in Dolphin et al. (2001), and what follows is only a summary. After obtaining the calibrated images from STScI, cosmic ray cleaning was performed with the HSTphot (Dolphin 2000a) *cleansep* routine which cleans images taken with different filters by allowing for a colour variation. Stellar photometry was then obtained with the HSTphot *multiphot* routine which measures magnitudes simultaneously in the two images, accounting for image alignment, WFPC2's wavelength-dependent plate scale, and geometric distortion. The fi-

[★] Based on observations made with the NASA/ESA Hubble Space Telescope. The Space Telescope Science Institute is operated by the Association of Universities for Research in Astronomy, Inc. under NASA contract NAS 5-26555. Based in part on observations obtained with the 6-m telescope operated by the Russian Academy of Sciences

^{**} Alfred P. Sloan Research Fellow

nal photometry was then done using aperture corrections to a $0''.5$ radius, and the Dolphin (2000b) charge-transfer inefficiency (CTE) correction and zero-point calibration applied. We estimate the aperture corrections in the three wide field chips to be accurate to 0.05 magnitude. The CTE correction depends on the X- and Y- positions, the background counts, the brightness of the stars, and the time of the observations. For our data the mean CTE correction makes a star brighter by $\sim 0^m.25$. Because of the small areal coverage of the Planetary Camera (PC) and consequent lack of stars suitable for an accurate aperture correction, the PC photometry is excluded from our analysis. Additionally, stars with a signal-to-noise ratio < 5 , $|\text{chi}| > 2.0$, or $|\text{sharpness}| > 0.4$ in each exposure were eliminated from the final photometry list, in order to minimize the number of false detections.

Finally, the F606W and F814W instrumental magnitudes of 1875 stars were converted to the standard V, I system following the "synthetic" transformations of Holtzman et al. (1995). We used the parameters of transformation from their Table 10, taking into account different relations for blue and red stars separately. Because we used the non-standard V filter F606W instead of F555W, the resulting I and especially V magnitudes may contain systematic errors. However, when comparing our F606W, F814W photometry of other snapshot targets with ground-based V, I photometry, we find that the transformation uncertainties, $\sigma(I)$ and $\sigma(V - I)$, are within $0^m.05$ for stars with colours of $0 < (V - I) < 2$. Note that the zero-point for the F606W observations is taken from WFPC2 observations of Omega Centauri as measured by Dolphin (2000b).

3. Colour-magnitude diagram and distance

Fig.3 shows the colour-magnitude diagrams (CMDs) derived for the central WF3 field, as well as for the neighbouring fields WF2 and WF4. In the central field the number of stars increases abruptly at $I \sim 22^m.3$, which we interpret as the tip of the red giant branch (TRGB). There are also some faint, bluish stars with $(V - I) < 0.5$ in the WF3. These stars may be indicative of a young population of KKR 25.

The magnitude of the TRGB has been obtained applying a Sobel filter. Following Sakai et al. (1996), we use an edge-detection filter, which is a modified version of a Sobel kernel $([-1, 0, +1])$, to the Gaussian-smoothed I-band luminosity function. Only red stars with colours $0.6 < (V - I) < 1.6$ were considered. The resulting luminosity function and the Sobel filtered luminosity function are shown in Fig. 4. The TRGB corresponds to the peak at $I = 22.32$ (bottom panel). The peak at $I = 22.7$ and several others are being produced by density fluctuations along the RGB. The error can be estimated as $1/2$ of the peak width at 62% of its maximum and turns out to be formally $0^m.10$.

According to Da Costa & Armandroff (1990), the TRGB can be assumed to be at $M_I = -4.05$ for metal-poor systems. With a Galactic extinction along the line of sight toward KKR 25 of $A_I = 0^m.02$ (Schlegel et al. 1998) this yields a distance modulus of $(m - M)_0 = 26^m.35 \pm 0^m.14$ or $D = 1.86 \pm 0.12$ Mpc. The quoted errors include the error in the TRGB detection ($0^m.10$), as well as uncertainties of the HST photometry zero point ($\sim 0^m.05$), the aperture corrections ($\sim 0^m.05$), and crowding effects ($\sim 0^m.06$) added in quadrature.

4. Results and discussions

The solid line in Fig. 3 (left panel) is the M15 globular cluster fiducial with $[\text{Fe}/\text{H}] = -2.2$ dex from Da Costa & Armandroff (1990), which was reddened and shifted to the derived galaxy's distance. This low-metallicity fiducial provides a good fit to the RGB of KKR 25. With knowledge of the distance modulus of KKR 25 we can estimate its mean metallicity from the mean colour of the RGB measured at an absolute magnitude $M_I = -3.5$, as recommended by Lee et al. (1993). Based on a Gaussian fit to the colour distribution of the giant stars in the range $22^m.6 < I < 23^m.0$ we derive a mean dereddened colour of the RGB stars of $(V - I)_{0, -3.5} = 1.26 \pm 0.07$. Following Lee et al. (1993) this yields a mean metallicity $[\text{Fe}/\text{H}] = (-2.1 \pm 0.3)$ dex.

Integrated photometry of the HST data of the galaxy was carried out with increasing circular apertures. The sky level was approximated by a two-dimensional polynomial, using regions with only a few stars near the edges of the images. Then the galaxy magnitude in each band was measured as the asymptotic value of the derived curve of growth. Fig. 5 shows the results.

A summary of the basic properties of KKR 25 is given in Table 1. The parameters listed in Table 1 are: (1,2) — equatorial coordinates of the galaxy center, (3) — morphological type, (4,5) — angular diameter along the major axis and axial ratio corresponding to a level of $B \sim 26.5^m/\square''$, (6) — Galactic extinction in V and I bands from Schlegel et al. (1998), (7,8) — integrated V magnitude and integrated colour, (9) — observed central surface brightness, (10) — apparent I magnitude of the RGB tip, (11) — true distance modulus, (12,13) — linear distance from the Milky Way and from the Local Group centroid, (14,15) — linear diameter and absolute magnitude, (16,17) — mean reddening-corrected colour of the RGB tip measured at an absolute magnitude $M_I = -3.5$, and corresponding mean metallicity, (18) — heliocentric velocity, (19) — radial velocity with respect to the Local Group centroid, (20) — HI line flux, (21) — HI line width, (22,23) — hydrogen mass-to-luminosity ratio and the dynamical (virial) mass-to-luminosity ratio determined in the same manner as in Huchtmeier et al. (2000).

As mentioned above, KKR 25 contains a population of faint bluish stars with $(V - I) < 0.5$. These stars are

distributed more or less homogeneously over the galaxy body. On August 2000 KKR 25 was imaged with the 6-m telescope with an H_α filter. After the subtraction of the continuum the H_α image shows no compact HII regions. These properties indicate that KKR 25 can be classified as a dIrr/dSph just as Phoenix and LGS 3.

We searched for globular clusters in KKR 25 and found one candidate situated half-way from the center to the left edge of WF3 (see Fig. 2). This bright diffuse object has an integrated apparent magnitude $V_T = 20.59$ and an angular half-light radius $r(0.5L) = 0''.58$ that corresponds to $M_V = -5^m.79$ and $R(0.5L) = 5.2$ pc, which are within the values typical of Galactic globular clusters. However, the integrated color of the object, $(V - I)_T = 1.83$, seems to be too red for a globular cluster.

According to its distance with respect to the Local Group centroid, $D_{LG} = 1.79$ Mpc, KKR 25 is situated beyond the radius of the zero-velocity surface for the Local Group (Karachentsev & Makarov 2001). The distance of KKR 25 is in good agreement with its positive radial velocity $V_{LG} = +72 \pm 2$ km/s with respect to the Local Group centroid. Note that the distance and the velocity of KKR 25 are almost the same as for another dIrr/dSph galaxy, Antlia, which has $D_{LG} = 1.70$ Mpc and $V_{LG} = +65$ km/s (Aparicio et al., 1997). Compared to Antlia, KKR 25 has a somewhat smaller luminosity and size. But unlike Antlia (associated with NGC 3109, Sex A, and Sex B), KKR 25 is a totally isolated object, with no other known galaxies within a radius of 0.5 Mpc.

Acknowledgements. Support for this work was provided by NASA through grant GO-08601.01-A from the Space Telescope Science Institute, which is operated by the Association of Universities for Research in Astronomy, Inc., under NASA contract NAS5-26555. I.D.K., V.E.K., and E.K.G. acknowledge partial support through the Henri Chrétien International Research Grant administered by the American Astronomical Society. D.G. acknowledges financial support for this project received from CONICYT through Fondecyt grant 8000002. This work has also been partially supported by the DFG-RFBR grant 01-02-04006 and RFBR grant 01-02-16001

References

- Aparicio A., Dalcanton J.J., Gallart C., Martinez-Delgado D., 1997, *AJ*, 114, 1447
- Da Costa G.S., Armandroff T.E., 1990, *AJ* 100, 162
- Dolphin A.E., 2000a, *PASP* 112, 1383
- Dolphin A.E., 2000b, *PASP* 112, 1397
- Dolphin A.E., Makarova L., Karachentsev I.D., Karachentseva V.E., Geisler D., Grebel E.K., Guhathakurta P., Hodge P.W., Sarajedini A., Seitzer P., 2001, *MNRAS*, 324, 249
- Grebel E.K., 2000, 33rd ESLAB Symposium on "Star Formation from the Small to the Large Scale", SP-445, eds. F.Favata, A.A.Kaas, & A.Wilson (Noordwijk: ESA), 87
- Holtzman J.A., Burrows C.J., Casertano S., et al, 1995, *PASP* 107, 1065
- Huchtmeier W.K., Karachentsev I.D., Karachentseva V.E., 2000, *A & AS*, 147, 187
- Karachentsev I.D., Karachentseva V.E., Suchkov A.A., Grebel E.K., 2000, *A & AS*, 145, 415
- Karachentsev I.D., Makarov D.I., 2001, *Astrofizika*, 44, 5
- Karachentseva V.E., Karachentsev I.D., 1998, *A & AS*, 127, 409
- Karachentseva V.E., Karachentsev I.D., Richter G.M., 1999, *A & AS*, 135, 221
- Karachentseva V.E., Karachentsev I.D., 2000, *A & AS*, 146, 359
- Lee M.G., Freedman W.L., Madore B.F., 1993, *ApJ* 417, 553
- Sakai S., Madore B.F., Freedmann W.L., 1996, *ApJ* 461, 713
- Schlegel D.J., Finkbeiner D.P., Davis M., 1998, *ApJ* 500, 525
- Whiting A.B., Irwin M.J., Hau G.K.T., 1997, *AJ*, 114, 996

Table 1. Observed and derived properties of KKR 25 in Draco

Parameter	KKR 25
R.A. (B1950.0)	$16^h 12^m 37.^s3$
Dec. (B1950.0)	$+54^\circ 29' 46''$
R.A. (J2000.0)	$16^h 13^m 47.^s7$
Dec. (J2000.0)	$+54^\circ 22' 15''$
Morphological type	dIrr/dSph
Angular diameter, $a_{26.5}$	$1'.1$
Axial ratio	0.59
Extinction, A_V/A_I	$0.^m03/0.^m02$
Total magnitude, V_T	$15.^m9 \pm 0.^m2$
$(V - I)_T$	0.88 ± 0.11
Central surface brightness, $\Sigma_{0,V}$	$24.^m0 \pm 0.^m2/\square''$
I_{TRGB}	$22.^m32 \pm 0.^m10$
$(m - M)_0$	$26.^m35 \pm 0.^m14$
Distance, D_{MW}	1.86 Mpc
Distance, D_{LG}	1.79 Mpc
Linear diameter, $A_{26.5}$	0.54 Kpc
Absolute magnitude, M_V	-10.48
$(V - I)_{0,-3.5}$	1.26 ± 0.07
[Fe/H]	$-2.1 \pm 0.3 \text{ dex}$
Heliocentric velocity, V_h	$-135 \pm 2 \text{ km/s}$
Corrected velocity, V_{LG}	$+72 \text{ km/s}$
HI flux	$2.20 \text{ Jy}\cdot\text{km/s}$
HI line width, W_{50}	14 km/s
$M(\text{HI})/L_V$	$0.80 M_\odot/L_\odot$
$M(\text{dyn})/L_V$	$1.50 M_\odot/L_\odot$

Fig. 1. *R*-band image of KKR 25 in Draco obtained with the 6m SAO telescope. The horizontal line corresponds to $10''$. North is up, and East to the left.

Fig. 2. WF3 image of KKR 25 produced by combining the two 600s exposures taken through the F606W and F814W filters. A globular cluster candidate is indicated by the arrow.

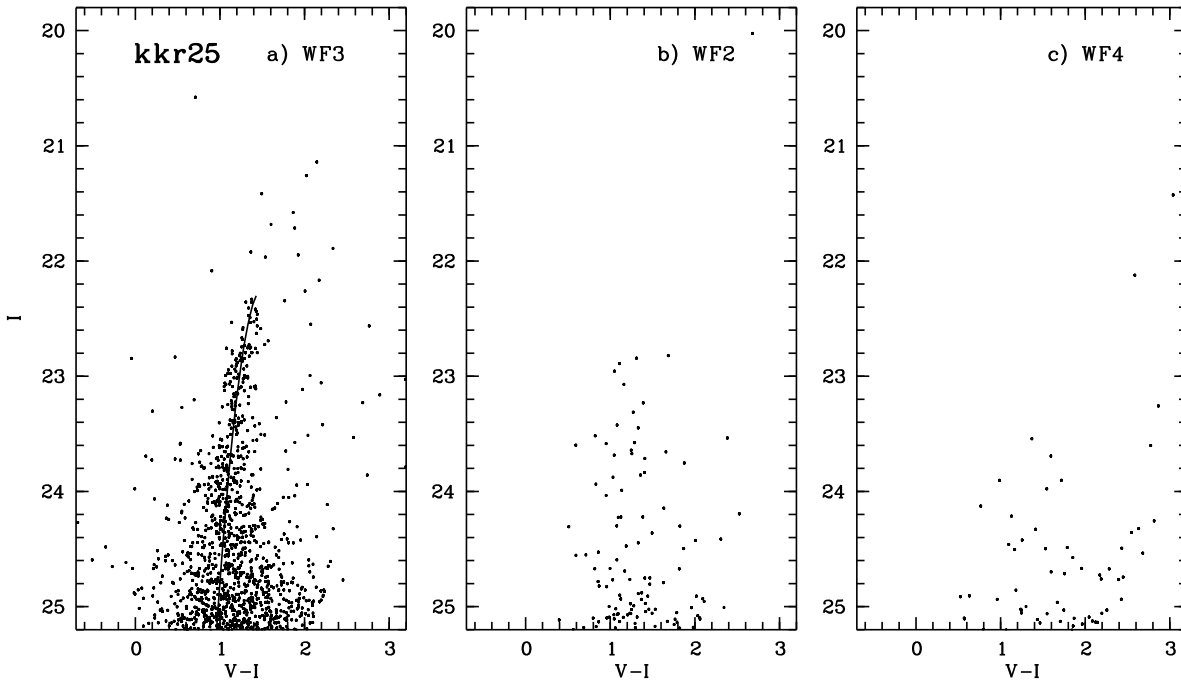


Fig. 3. WFPC2 colour-magnitude diagram for KKR 25 in Draco. The left panel shows stars in the WF3 chip, the middle and the right CMDs correspond to the WF2 and WF4 chips. The solid line in the left panel shows the red giant branch of the globular cluster M15 with metallicity of -2.17 dex.

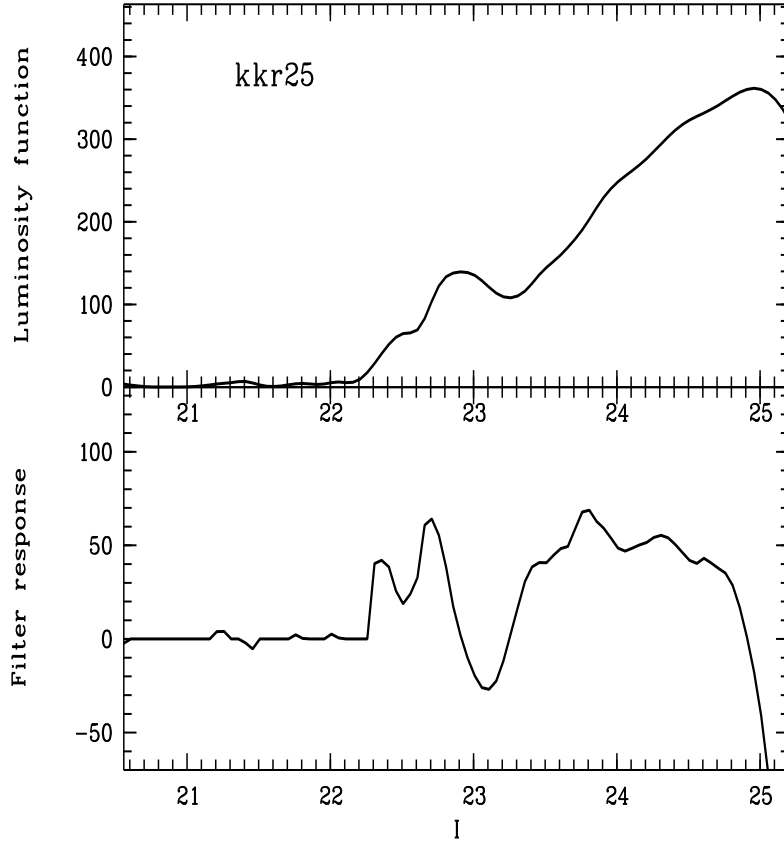


Fig. 4. The Gaussian-smoothed I-band luminosity function restricted to red stars with colors between $0.^m6 < (V-I) < 1.^m6$ (top), and the output of an edge-detection filter applied to the luminosity function (bottom) for KKR 25.

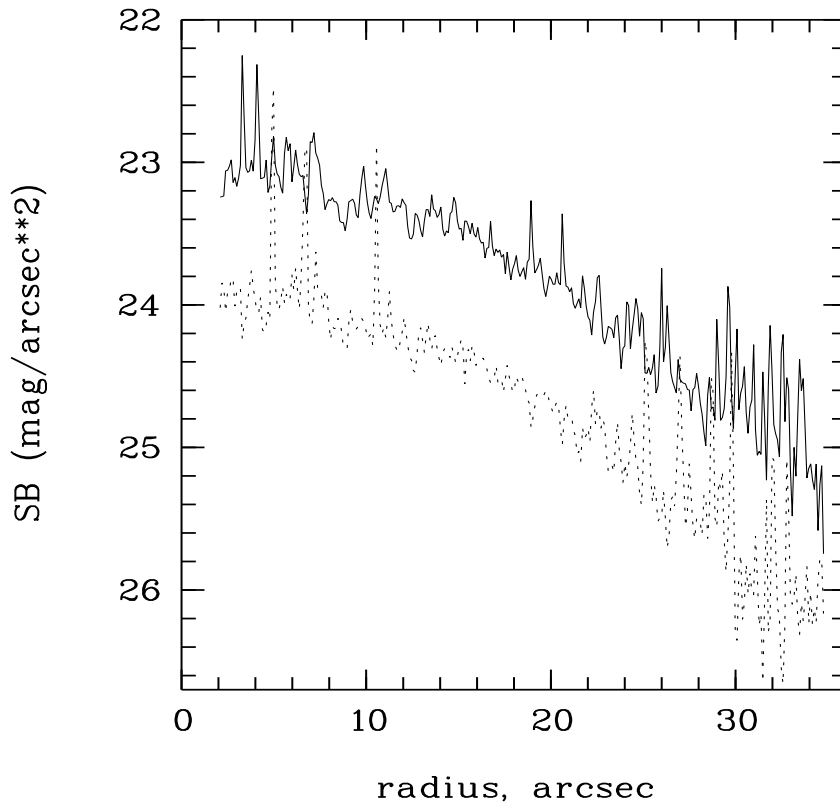


Fig. 5. Radial distribution of surface brightness in KKR 25 in the *V* (dashed) and the *I* (solid line) bands.

This figure "Draco_Fig1.jpg" is available in "jpg" format from:

<http://arxiv.org/ps/astro-ph/0110158v1>

This figure "Draco_Fig2.jpg" is available in "jpg" format from:

<http://arxiv.org/ps/astro-ph/0110158v1>